

Diffraction effects in planar wave-sphere interaction

Xiaowei Jia (贾晓伟), Jianqi Shen (沈建琪)*, Lufang Guo (郭露芳), and Chen Wan (万家)

College of Science, University of Shanghai for Science and Technology, Shanghai 200093, China

*Corresponding author: jqshen@163.com

Received December 14, 2012; accepted January 25, 2013; posted online April 19, 2013

Using the classical Mie scattering theory, we compute the energy density of an arbitrary partial wave (e.g., the n th order) and then determine that the interaction between an incident planar wave and a sphere of radius a is the one between the sphere and those partial waves the order of which satisfies $n \leq ka$. We also provide a simple expression to describe the diffracted wave in which the angle-dependent functions are employed. The difference between the accurate and the approximate expressions is demonstrated by numerical calculation.

OCIS codes: 050.1940, 290.4020.

doi: 10.3788/COL201311.050501.

Light diffraction occurs when light waves pass near the edge of an aperture or obstacle, causing waves to appear bent around the edge and interfere with forward-propagating light that misses the edge by a large distance^[1]. Classical diffraction theory is based on Kirchhoff's approximation, which leads to a well-defined formulation of the Huygens-Fresnel principle^[2]. The theory generates reasonable results for the diffraction patterns of apertures that have dimensions much larger than the wavelength for small diffraction angles θ , where most of the intensity is concentrated^[3]. For example, applying the theory to a circular aperture of radius a obtains the amplitude of the diffracted wave $S(\theta) = \alpha^2 \cdot J_1(\alpha \sin \theta) / (\alpha \sin \theta)$, where $\alpha = ka$ is the dimensionless size of the sphere and k is the wavenumber^[2]. This expression is applicable only for small angles; alternatively, the amplitude may be expressed as $S(\theta) = \frac{1+\cos\theta}{2} \alpha^2 J_1(\alpha \sin \theta) / (\alpha \sin \theta)$ ^[4] or as a matrix with the different polarization configurations of the diffracted wave^[5]. The latter expressions can be applied for backward-propagating diffracted waves (for diffraction angles larger than 90°) because of the angular factor $\cos\theta$. The differences between these expressions are attributed to the approximations generated during deduction. Studies on diffraction have recently been published^[6,7]. We revisit diffraction effects by using the classical Mie scattering theory and then demonstrating planar wave-sphere interaction. A simple expression is provided to describe the diffracted wave in which angle-dependent functions are employed. An approximate expression is obtained to verify whether the results agree with those deduced from Kirchhoff's approximation. Numerical calculation is performed to demonstrate how the difference between the accurate and the approximate expressions occurs.

The classical Mie theory describes the interaction between an incident planar wave and a sphere, as shown in Fig. 1.

In the time convention of $\exp(-i\omega t)$, the incident planar wave $\mathbf{E}_{\text{inc}} = E_0 \exp(ikz)\hat{\mathbf{e}}_x$ is expressed as a series of partial waves given as

$$\mathbf{E}_{\text{inc}} = \sum_{n=1}^{\infty} \mathbf{E}_{\text{inc},n}, \quad (1)$$

$$\mathbf{H}_{\text{inc}} = \sum_{n=1}^{\infty} \mathbf{H}_{\text{inc},n}, \quad (2)$$

$$\mathbf{E}_{\text{inc},n} = E_0 i^n \frac{2n+1}{n(n+1)} (\mathbf{M}_{\text{o}1n}^{(1)} - i\mathbf{N}_{\text{e}1n}^{(1)}), \quad (3)$$

$$\mathbf{H}_{\text{inc},n} = -\frac{k}{\omega\mu} E_0 i^n \frac{2n+1}{n(n+1)} (\mathbf{M}_{\text{e}1n}^{(1)} + i\mathbf{N}_{\text{o}1n}^{(1)}), \quad (4)$$

where $\mathbf{M}_{\text{o}1n}^{(1)}$, $\mathbf{M}_{\text{e}1n}^{(1)}$, $\mathbf{N}_{\text{e}1n}^{(1)}$, and $\mathbf{N}_{\text{o}1n}^{(1)}$ are the vector spherical harmonics^[4], $k (= 2\pi/\lambda)$ is the wave number, λ is the wavelength, ω is the angular frequency of the wave, μ is the magnetic permeability of the medium, and E_0 is the magnitude of the electric field. The average energy density of an arbitrary partial wave (say the n th order) is given as^[8,9]

$$\begin{aligned} W_{\text{inc},n} &= \frac{\varepsilon}{4} |\mathbf{E}_{\text{inc},n}|^2 + \frac{\mu}{4} |\mathbf{H}_{\text{inc},n}|^2 \\ &= \frac{\varepsilon}{2} E_0^2 (2n+1)^2 \left[\sin^2 \theta \pi_n^2(\theta) \frac{\psi_n^2(\rho)}{\rho^4} \right. \\ &\quad \left. + \frac{\pi_n^2(\theta) + \tau_n^2(\theta)}{n^2(n+1)^2} \frac{\psi_n^2(\rho) + \psi_n'^2(\rho)}{\rho^2} \right], \quad (5) \end{aligned}$$

where ε is the electric constant of the medium, $\psi_n(\rho)$ is the Riccati-Bessel function of the 1st kind (the argument is $\rho = kr$) and $\psi_n'(\rho)$ is its derivative. $\pi_n(\theta)$ and $\tau_n(\theta)$ are the angle-dependent functions defined as

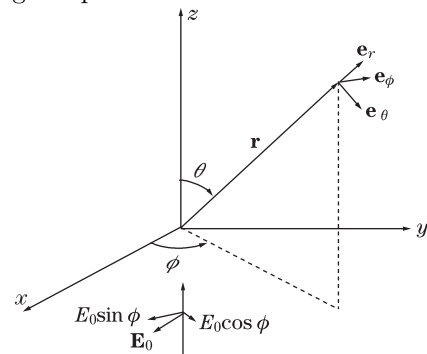


Fig. 1. Interaction between an incident planar wave and a sphere.

$$\pi_n(\theta) = \frac{P_n^1(\cos \theta)}{\sin \theta}, \quad (6)$$

$$\tau_n(\theta) = \frac{d}{d\theta} P_n^1(\cos \theta), \quad (7)$$

where $P_n^1(\cos \theta)$ is the associated Legendre function.

Equation (5) indicates that the energy density of the partial wave is axially symmetric around z -axis. The numerical results of the energy density of the partial wave are plotted in the yz plane, as shown in Fig. 2, in which the orders of the partial wave n are 500 and 1 000. The calculation method used in this letter is based on a procedure applied in a previous study^[8,9]. For the partial wave of n , the energy is mainly distributed in the region $\rho = kr > n$, which suggests that the n th partial wave does not reach the region $\rho = kr < n$. Therefore, the interaction between an incident planar wave and a sphere of radius a is the same with that between the sphere and those partial waves the order of which satisfies $n < \alpha = ka$. By contrast, the partial waves of $n \geq \alpha = ka$ do not interact with the sphere. This result agrees with the localization principle given by Hulst^[10]. According to the localization principle, the term of the order n corresponds to a ray passing through the origin at a distance $(n + 1/2)/k$, and the terms with $n + 1/2 \leq \alpha = ka$ correspond to all rays reaching the sphere. In the view of quantum mechanics, the wavelength of a photon is $\lambda = h/p$, where h is Planck's constant and p is the momentum. For the sphere with the radius a , the angular momentum $nh/2\pi$ must not exceed pa , thus setting the condition $n \leq 2\pi a/\lambda = \alpha$. Given that the order of the partial wave n is discrete and the size parameter α changes continuously, $n \leq \alpha - 1/2$ in the average may be chosen. The discussion above also explains the criterion of the stopping order in Mie scattering calculation given by Wiscombe *et al.*, which includes the edge domain^[11–13].

According to the Debye series expansion of Mie scattering, the scattering field can be considered as the interference involving three parts: the diffracted light, the light reflected by the incident ray on the surface of the sphere, and the light wave with multiple internal reflections^[13–15]. The diffracted wave can be expressed as

$$\mathbf{E}_{\text{diff}} = \frac{1}{2} \sum_{n=1}^{n_s} E_n (\mathbf{iN}_{e1n}^{(3)} - \mathbf{M}_{o1n}^{(3)}), \quad (8)$$

$$\mathbf{H}_{\text{diff}} = \frac{k}{2\omega\mu} \sum_{n=1}^{n_s} E_n (\mathbf{iN}_{o1n}^{(3)} + \mathbf{M}_{e1n}^{(3)}), \quad (9)$$

where $n_s = \text{int}(\alpha - 1/2)$. $\mathbf{M}_{e1n}^{(3)}$, $\mathbf{M}_{o1n}^{(3)}$, $\mathbf{N}_{e1n}^{(3)}$ and $\mathbf{N}_{o1n}^{(3)}$ are the vector spherical harmonics, which describe the outward wave in the time convention of $\exp(-i\omega t)$ ^[4]. In the far-field diffraction limit, Eq. (8) can be simplified as

$$\mathbf{E}_{\text{diff}} = -\frac{\exp(i\rho)}{i\rho} E_0 S \hat{\mathbf{e}}_{\text{diff}}, \quad (10)$$

$$S = \frac{1}{2} \sum_{n=1}^{n_s} \frac{2n+1}{n(n+1)} [\pi_n(\theta) + \tau_n(\theta)], \quad (11)$$

$$\hat{\mathbf{e}}_{\text{diff}} = \cos \phi \hat{\mathbf{e}}_\theta - \sin \phi \hat{\mathbf{e}}_\phi, \quad (12)$$

where S is the amplitude function describing the diffracted wave. The expression above indicates that the far-field diffracted wave is transversal and linearly polarized, with its intensity given as

$$I_{\text{diff}} = \frac{1}{\rho^2} I_0 |S|^2, \quad (13)$$

where I_0 is the intensity of the incident planar wave. By using the recurrence of the angle-dependent functions^[4], Eq. (11) may be further simplified to

$$S(\theta) = (1 + \cos \theta) \pi_{n_s}(\theta) - \frac{1}{2} \frac{n_s + \cos \theta}{n_s + 1} \pi_{n_s}(\theta) - \frac{1}{2} \pi_{n_s-1}(\theta). \quad (14)$$

Deduced from the Debye series expansion of Mie scattering theory, Eq. (14) can accurately describe diffraction. For large spheres (i.e., $n_s \gg 1$), the angle-dependent function satisfies $\pi_{n_s-1}(\theta) \approx \cos \theta \pi_{n_s}(\theta)$ in the range $\alpha \sin \theta < 10$. Thus, Eq. (14) may be approximated to

$$S(\theta) \approx \frac{1 + \cos \theta}{2} \pi_{n_s}(\theta). \quad (15)$$

Applying the approximation of the angle-dependent function $\pi_{n_s}(\theta) \approx n_{s+}^2 J_1(n_{s+} \sin \theta) / n_{s+} \sin \theta$ (here $n_{s+} = n_s + 1$) to Eq. (15), we obtain

$$S(\theta) \approx \frac{1 + \cos \theta}{2} n_{s+}^2 \cdot \frac{J_1(n_{s+} \sin \theta)}{n_{s+} \sin \theta}. \quad (16)$$

If n_{s+} is replaced by α , the approximate expression of the diffraction given in Eq. (16) coincides with the one obtained from the scalar diffraction theory by Bohren *et al.*^[4]. Although the relationship $\pi_{n_s-1}(\theta) \approx \cos \theta \cdot \pi_{n_s}(\theta)$ exists in both the forward and backward directions, the approximation of Eq. (15) may cause big errors in the backward direction because the factor $(1 + \cos \theta)/2$ tends to approach 0, which is the same case as Eq. (16). Therefore, the approximations in Eqs. (15) and (16) can yield good results only in the range $\theta < \arcsin(10/\alpha)$.

The approximation from Eqs. (15) and (16) exists in the range of forward directions (i.e., $\alpha \sin \theta < 10$ and $\theta < 90^\circ$). Comparison between the numerical results calculated using Eqs. (14), (15), and (16) is given in Fig. 3. The diffraction of light is expressed as $|S(\theta)|^2$ for the sphere with the size $\alpha = 30$. In the range $\theta < 19.5^\circ$, the result obtained from Eq. (15) is in agreement with that obtained from Eq. (14), as shown in Fig. 3(a). In all

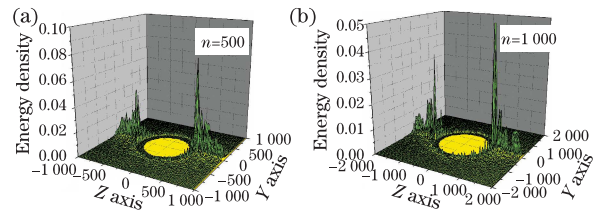


Fig. 2. (Color online) Distributions of the energy density of the partial waves for (a) $n = 500$ and (b) $n = 1000$. $Y = \rho \sin \theta$ and $Z = \rho \cos \theta$.

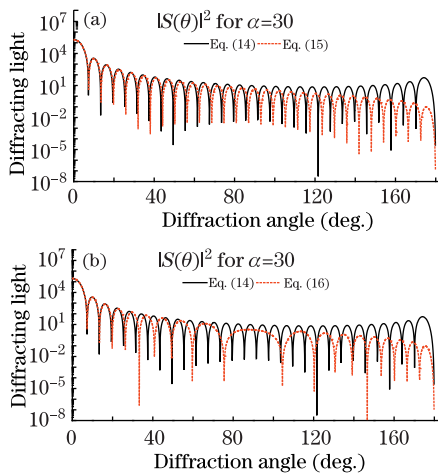


Fig. 3. (Color online) Comparison of diffracted intensity $|S(\theta)|^2$ calculated using Eqs. (14), (15), and (16), with $\alpha = 30$ and $n_s = 29$.

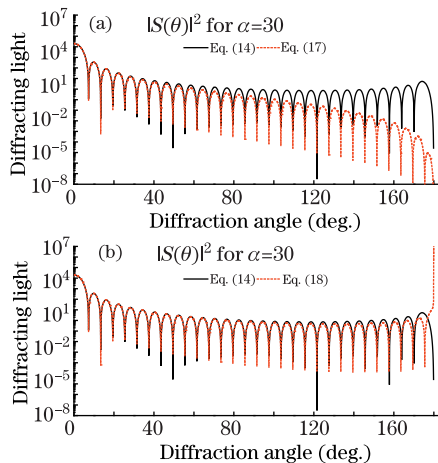


Fig. 4. (Color online) Comparison of the results calculated with Eqs. (14), (17), and (18), with $\alpha = 30$ and $n_s = 29$.

ranges of diffraction angles, both curves oscillate uniformly with the variation in the diffraction angle; however, the frequency of oscillations vary. This difference is attributed to the oscillation of the angular-dependent function $\pi_{n_s}(\theta)$ at a frequency that is dependent on the order. Thus, the approximation $\pi_{n_s-1}(\theta) \approx \cos\theta \cdot \pi_{n_s}(\theta)$ changes the oscillating properties. In addition, as the diffraction angle increases, the results increasingly deviate from each other.

The results obtained from Eqs. (14) and (16) agree well in the forward direction (i.e., $\theta < 19.5^\circ$) and deviate increasingly from each other with the increase in the diffraction angle. In addition, the curve defined by Eq. (16) oscillates rapidly in the ranges in forward and backward directions and oscillates slowly in the vicinity of $\theta = 90^\circ$ because of the approximation $\pi_{n_s}(\theta) \approx n_{s+}^2 \cdot J_1(n_{s+} \sin\theta)/(n_{s+} \sin\theta)$. This change occurs because the angular-dependent function $\pi_{n_s}(\theta)$ is related to the associated Legendre function, which is obtained under spherical conditions, whereas the Bessel function is obtained in the circular disk conditions. This difference indicates that the dependence of the oscillating properties of these functions on the diffraction an-

gle varies. The oscillation properties of the diffraction light by the diffraction angle can be modified by substituting $J_1(n_{s+} \sin\theta)/(n_{s+} \sin\theta)$ with $J_1(n_{s+}\theta)/(n_{s+}\theta)$. In addition, the associated Legendre function describes the standing wave in the sphere, and the Bessel function describes the standing wave in the circular disk. In the range of $\theta \in [0, \pi]$, $\pi_{n_s}(\theta) \propto (2\pi \sin\theta)^{-\frac{1}{2}}$, and $J_1(n_{s+}\theta)/n_{s+}\theta \propto (2\pi\theta)^{-\frac{1}{2}}$. Thus, the approximation $\pi_{n_s}(\theta) \approx n_{s+}^2 \cdot J_1(n_{s+} \sin\theta)/(n_{s+} \sin\theta)$ above can be modified to $\pi_{n_s}(\theta) \approx n_{s+}^2 \cdot (\theta/\sin\theta)^{\frac{1}{2}} \cdot J_1(n_{s+}\theta)/(n_{s+}\theta)$. An equation corresponding to Eq. (16) can be written as

$$S(\theta) \approx \frac{1 + \cos\theta}{2} n_{s+}^2 \cdot \left(\frac{\theta}{\sin\theta}\right)^{\frac{1}{2}} \frac{J_1(n_{s+}\theta)}{n_{s+}\theta}. \quad (17)$$

The numerical result is shown in Fig. 4(a) for comparison with the one calculated using Eq. (14). The result in Eq. (17) deviates from that in Eq. (14) for large diffraction angles because of the approximation derived from deducing Eq. (15) from Eq. (14). Therefore, by simply omitting the factor $(1 + \cos\theta)/2$, the expression can be rewritten as

$$S(\theta) \approx n_{s+}^2 \left(\frac{\theta}{\sin\theta}\right)^{\frac{1}{2}} \frac{J_1(n_{s+}\theta)}{n_{s+}\theta}. \quad (18)$$

To a certain extent, Eq. (18) is equivalent to the expression given by Nussenzveig *et al.* from the semi-classical diffraction theory^[3,14–16]. As shown in Fig. 4(b), the numerical result of Eq. (18) matches well that of Eq. (14), except for the angles very close to $\theta = 180^\circ$, wherein the $\theta/\sin\theta$ value tends to be infinite. The excellent consistency between the results of Eqs. (14) and (18) implies that the omission of the factor $(1 + \cos\theta)/2$ compensates for the approximation in Eq. (15).

Numerical calculations for Eqs. (14), (17), and (18) are performed with different size parameters, which exhibit the same characteristics as those in Figs. 3 and 4. The results of Eqs. (14) and (18) remain in agreement when the size parameter is set to as low as $\alpha = 5$.

Finally, although Eq. (14) is derived rigorously from the Debye series expansion of Mie scattering, the equation cannot reflect the slight change in α . For example, the maximal order $n_s = 29$ remains unchanged for all particle size parameters in the range of $\alpha \in [29.5, 30.5]$. The midpoint of the range is $n_{s+} = 30$. With this consideration, Eq. (18) can be further modified to obtain

$$S(\theta) \approx \alpha^2 \cdot \left(\frac{\theta}{\sin\theta}\right)^{\frac{1}{2}} \frac{J_1(\alpha\theta)}{\alpha\theta}. \quad (19)$$

In conclusion, the diffraction of a planar wave by a sphere is discussed from the perspective of the classical Mie scattering theory. In the first step, the planar wave is considered an interference of partial waves with different orders. The distribution of the field energy of a partial wave is calculated. The calculation determines that only partial waves with orders lower than the dimensionless size of the sphere (i.e., $n < \alpha$) contribute to the interaction between the planar wave and the sphere. In the second step, the expression for diffraction light is deduced from the Debye series expansion. The far-field diffracted

wave is found to be transversely and linearly polarized. Finally, different approximations of the diffraction light are obtained, i.e., Eqs. (15)–(19), and compared with those obtained from scalar diffraction theory and semi-classical diffraction theory. Numerical calculations with these approximations are plotted, hence, the comparison with the rigorous calculation obtained from Mie theory (i.e., Eq. (14)). Among these approximations, Eqs. (18) and (19) provide the most accurate results, except for angles that are very close to $\theta = 180^\circ$.

We explain light diffraction from interactions between partial waves and a sphere. The approximation obtained may be applied in geometrical optics approximation of light scattering^[5,17,18] and other areas.

This work was supported by the National Natural Science Foundation of China (No. 50876069), the Innovation Program of Shanghai Municipal Education Commission (No. 12ZZ136), and the Specialized Research Fund for the Doctoral Program of Higher Education (No. 20093120110006).

References

1. D. Halliday, R. Resnick, and J. Walker, *Fundamentals of Physics* (Wiley, New York, 2005).
2. M. Born and E. Wolf, *Principles of Optics* (Cambridge University Press, Cambridge, 2005).
3. H. M. Nussenzveig, *Diffraction Effects in Semiclassical Scattering* (Cambridge University Press, Cambridge, 1992).
4. C. F. Bohren and D. R. Huffman, *Absorption and Scattering of Light by Small Particles* (Wiley, New York, 1983).
5. P. Yang and K. N. Liou, *Contr. Atmos. Phys.* **71**, 223 (1998).
6. J. A. Lock and P. Laven, *J. Opt. Soc. Am. A* **28**, 1096 (2011).
7. W. Guo, *J. Opt. Soc. Am. A* **27**, 492 (2010).
8. A. Bott and W. Zdunkowski, *J. Opt. Soc. Am. A* **4**, 1361 (1987).
9. R. Ruppin, *J. Opt.* **13**, 095101 (2011).
10. H. C. van de Hulst, *Light Scattering by Small Particles* (Dover, New York, 1981).
11. W. J. Wiscombe, *Appl. Opt.* **19**, 1505 (1980).
12. J. Shen and X. Cai, *PIERS Online* **1**, 691 (2005).
13. H. M. Nussenzveig and W. J. Wiscombe, *Phys. Rev. A* **43**, 2093 (1991).
14. E. A. Hovenac and J. A. Lock, *J. Opt. Soc. Am. A* **9**, 781 (1992).
15. H. M. Nussenzveig, *J. Phys. A* **21**, 81 (1988).
16. Frank W. J. Olver, *Asymptotics and Special Functions* (Academic, New York, 1974).
17. H. Yu, J. Shen, and Y. Wei, *Particuology* **6**, 340 (2008).
18. H. Yu, J. Shen, and Y. Wei, *J. Quantum Spectum Rad. Tran.* **110**, 1178 (2009).